Vol 16 No 3, March 2007
1009-1963/2007/16(03)/0766-06

Chinese Physics

© 2007 Chin. Phys. Soc.
and IOP Publishing Ltd

Theoretical analysis of a relativistic travelling wave tube filled with plasma*

Xie Hong-Quan(谢鸿全)[a)†] and Liu Pu-Kun(刘濮鲲)[b)]

[a)] *School of Science, Southwest University of Science and Technology, Mianyang* 621010, *China*

[b)] *Institute of Electronics, Chinese Academy of Sciences, Beijing* 100080, *China*

(Received 30 November 2005; revised manuscript received 11 October 2006)

A cold and uniform plasma-filled travelling wave tube with sinusoidally corrugated slow wave structure is driven by a finite thick annular intense relativistic electron beam with the entire system immersed in a strong longitudinal magnetic field. By means of the linear field theory, the dispersion relation for the relativistic travelling wave tube (RTWT) is derived. By numerical computation, the dispersion characteristics of the RTWT are analysed in different cases of various geometric parameters of the slow wave structure and plasma densities. Also the gain versus frequency for three different plasma densities and the peak gain of the tube versus plasma density are analysed. Some useful results are obtained on the basis of the discussion.

Keywords: RTWT, plasma, annular electron beam, dispersion characteristic, gain
PACC: 5235, 5240D, 5275

1. Introduction

Relativistic travelling wave tube (RTWT) is an important high-power microwave (HPM) apparatus which has been developed in the past twenty years.[1−12] An amplifier is driven by the interaction of a slow space charge wave propagating on an electron beam with an electromagnetic wave supported by the slow wave structure (SWS). It can amplify the high-frequency signal and can be applied to the cyclotron resonance heating of fusion plasmas, drivers for new-generation high-energy electron accelerators and phased array radars due to the characteristics of high power and broad bandwidth. Recently, it has been found experimentally that injecting plasma into the microwave apparatus can enhance the interaction efficiency and the output power much more than the vacuum case. Plasma also can improve the transmission quality of electron beam so much as making beam transmit without a guiding magnetic field. Therefore, much attention has been attracted to this area of plasma-filled high-power microwave devices. All-Russian Electrotechnical Institute (VEI), Moscow, developed plasma-filled coupled cavity TWTs.[13] Hughes Research Laboratories developed the plasma-assisted slow wave oscillator (PASOTRON).[12] It can be modified for operation as a TWT. University of Maryland developed plasma generation and characterization techniques. Their theoretical studies showed that plasma-filled TWTs can have much higher gain than vacuum counterparts.[5] At first, their researches focused on the backward wave oscillator.[13−16] Then researches of TWT filled with plasma have been reported gradually.[3−5] At present, many researches in this area have been carried out also in Institute of High Energy Electronics, University of Electronic Science and Technology of China.[6−11]

In this paper, a cold and uniform plasma-loaded RTWT with sinusoidally corrugated SWS is studied. The dispersion relation of sinusoidally corrugated SWS is derived from a rigorous solution of the field equations. By numerical computation, the dispersion characteristics of the RTWT are analysed in detail in different cases of various geometric parameters of slow wave structure and plasma densities. Some useful results are obtained on the basis of the analysis.

In Section 2, the physical model of the RTWT filled with plasma is established in an infinite longitudinal magnetic field. In Section 3, the dispersion relation of the sinusoidally corrugated slow wave structure is derived. In Section 4, the dispersion characteristics

*Project supported by the National Natural Science Foundation of China (Grant No 10347009) and Science Foundation of Education Bureau of Sichuan Province, China (Grand No 2003B019).

†E-mail: hongquanxie@263.net

of the RTWT are analysed by numerical computation.

2. Physical model

The analysis presented in this paper is based on the SWS shown in Fig.1. The SWS consists of an axially symmetric, cylindrical waveguide whose wall radius, $R(z)$, varies sinusoidally according to the relation

$$R(z) = R_0 + h\cos(k_0 z), \tag{1}$$

where h is the corrugation amplitude, $k_0 = 2\pi/z_0$ is the corrugation wave number, and z_0 is the length of the corrugation period.

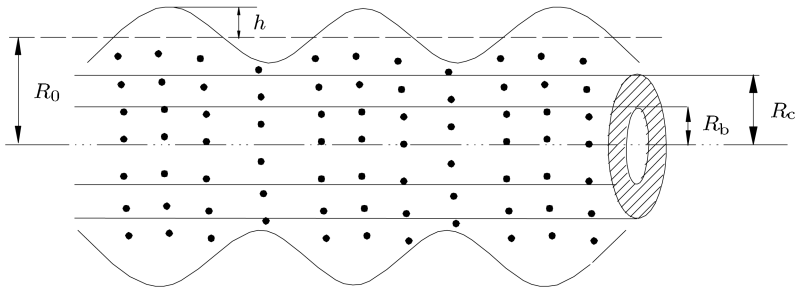


Fig.1. Slow wave structure and beam model of a relativistic travelling wave tube.

A finite thick annular intense relativistic electron beam with density n_b, inner radius R_b and outer radius R_c goes through the waveguide, which is loaded completely with a cold, uniform, collisionless plasma of density n_p. The entire system is immersed in a strong, longitudinal magnetic field, which magnetizes both the beam and the plasma.

The plasma is an anisotropic dielectric in the magnetic field. In the beam-plasma case in a linearized scheme of treatment, the dielectric tensor, in cylindrical coordinates, may be given by[17−19]

$$[\varepsilon] = \varepsilon_0 \begin{bmatrix} \varepsilon_1 & \varepsilon_2 & 0 \\ -\varepsilon_2 & \varepsilon_1 & 0 \\ 0 & 0 & \varepsilon_3 \end{bmatrix}, \tag{2}$$

where

$$\varepsilon_1 = 1 - \omega_\mathrm{p}^2/(\omega^2 - \omega_\mathrm{c}^2), \tag{3}$$

$$\varepsilon_2 = \mathrm{i}\omega_\mathrm{p}^2\omega_\mathrm{c}/[\omega(\omega^2 - \omega_\mathrm{c}^2)], \tag{4}$$

$$\varepsilon_3 = 1 - \omega_\mathrm{p}^2/[\gamma^3(\omega - k_n v)^2]. \tag{5}$$

Here, $\omega_\mathrm{p} = (e^2 n_\mathrm{p}/\varepsilon_0 m)^{1/2}$ is the plasma frequency, $\omega_\mathrm{b} = (e^2 n_\mathrm{b}/\varepsilon_0 m)^{1/2}$ is the beam plasma frequency, $\omega_\mathrm{c} = eB_0/m$ is the electron cyclotron frequency, ω is the angular frequency of the electromagnetic wave, γ is the relativistic factor, $k_n = k_z + nk_0$, where k_z is the axial wave number, and v is the electron beam velocity. To avoid the coupling of the TE and the TM modes, we assume that B_0 is so strong that $|\varepsilon_2|$ is negligibly small and $\varepsilon_1 = 1$.

3. Dispersion equation

In the above physical model, its Maxwell equations can be written as

$$\nabla \times \boldsymbol{H} = \frac{\partial \boldsymbol{D}}{\partial t}, \tag{6}$$

$$\nabla \times \boldsymbol{E} = -\frac{\partial \boldsymbol{B}}{\partial t}, \tag{7}$$

$$\nabla \cdot \boldsymbol{B} = 0, \tag{8}$$

$$\nabla \cdot \boldsymbol{D} = 0. \tag{9}$$

From Eqs.(6) and (7) we can obtain

$$\nabla(\nabla \cdot \boldsymbol{E}) - \nabla^2 \boldsymbol{E} = -\mu_0 \frac{\partial^2 \boldsymbol{D}}{\partial t^2}. \tag{10}$$

Suppose that every variable can be regarded as

$$\boldsymbol{A} = \boldsymbol{A}\mathrm{e}^{\mathrm{i}(k_n z - \omega t)}. \tag{11}$$

Equation (10) may be written as

$$\nabla(\nabla \cdot \boldsymbol{E}) - \nabla^2 \boldsymbol{E} = \frac{\omega^2}{c^2}\boldsymbol{\varepsilon}_r \cdot \boldsymbol{E}. \tag{12}$$

Substituting Eq.(2) into Eq.(12) and taking into account the longitudinal electric field, we have

$$\nabla^2 \boldsymbol{E}_z - [\nabla(\nabla \cdot \boldsymbol{E})]_z + \frac{\omega^2}{c^2}\varepsilon_3 \boldsymbol{E}_z = 0. \tag{13}$$

Substituting Eq.(2) into Eq.(9), we obtain

$$\nabla \cdot \boldsymbol{E} = \frac{\partial}{\partial z} E_z \Big[\frac{\omega_{\rm p}^2}{\omega^2} + \frac{\omega_{\rm b}^2}{\gamma^3(\omega - k_n v)^2}\Big]. \tag{14}$$

From Eqs.(13) and (14), we have

$$\nabla_\perp^2 E_z + \Big(\frac{\omega^2}{c^2} - k_n^2\Big) \times \Big[1 - \frac{\omega_{\rm p}^2}{\omega^2} - \frac{\omega_{\rm b}^2}{\gamma^3(\omega - k_n v)^2}\Big] E_z = 0, \tag{15}$$

where

$$\nabla_\perp^2 = \nabla^2 - \frac{\partial^2}{\partial z^2}. \tag{16}$$

For the periodical SWS, the field components should be expanded into space harmonics according to Floquet's theorem:

$$E_z(r,z) = \sum_{n=-\infty}^{\infty} E_{zn}(r) {\rm e}^{{\rm i}(k_n z - \omega t)}, \tag{17}$$

$$E_r(r,z) = \sum_{n=-\infty}^{\infty} \frac{{\rm i} k_n}{\omega^2/c^2 - k_n^2} {\rm e}^{{\rm i}(k_n z - \omega t)} \frac{{\rm d}E_{zn}}{{\rm d}r}. \tag{18}$$

Substituting Eq.(17) into Eq.(15) we can obtain

$$E_{zn} = \begin{cases} A_n J_0(T_1 r), & 0 \le r \le R_{\rm b}; \\ B_n J_0(T_2 r) + C_n N_0(T_2 r), & R_{\rm b} \le r \le R_{\rm c}; \\ D_n J_0(T_1 r) + F_n N_0(T_1 r), & R_{\rm c} \le r \le R(z); \end{cases} \tag{19}$$

where

$$T_1^2 = \Big(\frac{\omega^2}{c^2} - k_n^2\Big)\Big(1 - \frac{\omega_{\rm p}^2}{\omega^2}\Big), \tag{20}$$

$$T_2^2 = \Big(\frac{\omega^2}{c^2} - k_n^2\Big)\Big[1 - \frac{\omega_{\rm p}^2}{\omega^2} - \frac{\omega_{\rm b}^2}{\gamma^3(\omega - k_n v)^2}\Big]. \tag{21}$$

The field components must satisfy the following continuity equations:

$$E_z(r = R_{\rm b}^-) = E_z(r = R_{\rm b}^+), \tag{22}$$

$$E_z(r = R_{\rm c}^-) = E_z(r = R_{\rm c}^+), \tag{23}$$

$$E_r(r = R_{\rm b}^-) = E_r(r = R_{\rm b}^+), \tag{24}$$

$$E_r(r = R_{\rm c}^-) = E_r(r = R_{\rm c}^+). \tag{25}$$

From Eqs.(18) through (25) we have

$$B_n = -\frac{\pi}{2} R_{\rm b} K_n A_n, \tag{26}$$

$$C_n = -\frac{\pi}{2} R_{\rm b} L_n A_n, \tag{27}$$

$$D_n = \frac{\pi^2}{4} R_{\rm b} R_{\rm c} R_n A_n, \tag{28}$$

$$F_n = \frac{\pi^2}{4} R_{\rm b} R_{\rm c} T_n A_n, \tag{29}$$

where

$$K_n = T_2 J_0(T_1 R_{\rm b}) N_1(T_2 R_{\rm b}) - T_1 J_1(T_1 R_{\rm b}) N_0(T_2 R_{\rm b}), \tag{30}$$

$$L_n = T_1 J_1(T_1 R_{\rm b}) J_0(T_2 R_{\rm b}) - T_2 J_0(T_1 R_{\rm b}) J_1(T_2 R_{\rm b}), \tag{31}$$

$$R_n = K_n[T_1 J_0(T_2 R_{\rm c}) N_1(T_1 R_{\rm c}) - T_2 J_1(T_2 R_{\rm c}) N_0(T_1 R_{\rm c})] + L_n[T_1 N_0(T_2 R_{\rm c}) N_1(T_1 R_{\rm c}) - T_2 N_1(T_2 R_{\rm c}) N_0(T_1 R_{\rm c})] \tag{32}$$

$$T_n = K_n[T_2 J_1(T_2 R_{\rm c}) J_0(T_1 R_{\rm c}) - T_1 J_1(T_1 R_{\rm c}) J_0(T_2 R_{\rm c})] + L_n[T_2 N_1(T_2 R_{\rm c}) J_0(T_1 R_{\rm c}) - T_1 N_0(T_2 R_{\rm c}) J_1(T_1 R_{\rm c})]. \tag{33}$$

At the perfectly conducting corrugated waveguide surface, the tangential electric field must be zero,

$$E_z(r = R(z)) + E_r(r = R(z)) \frac{{\rm d}R(z)}{{\rm d}z} = 0. \tag{34}$$

Substituting the expressions for the axial and radial RF electric fields into Eq.(34), the dispersion relation is derived from the requirement for the existence of a nontrivial set of solutions of amplitudes A_n.

Equation (34) is a dispersion relation between ω and k_z. To eliminate z and unknown coefficients A_n, Eq.(34) is multiplied by ${\rm e}^{-{\rm i}mk_0 z}$ and integrated from $z = -\pi/k_0$ to $z = \pi/k_0$. The resulting dispersion relation is

$$\sum_{n=-\infty}^{\infty} A_n \int_{-\pi/k_0}^{\pi/k_0} {\rm e}^{{\rm i}(n-m)k_0 z} \Big(1 + \frac{{\rm i}k_n}{\omega^2/c^2 - k_n^2} \frac{\rm d}{{\rm d}z}\Big) \times [R_n J_0(T_1 R(z)) + T_n N_0(T_1 R(z))] {\rm d}z = 0. \tag{35}$$

To solve Eq.(35), $J_0(T_1 R(z))$ and $N_0(T_1 R(z))$ are expanded in Taylor series about $R(z) = R_0$.

$$J_0(T_1 R(z)) = \sum_{q=0}^{\infty} \frac{J_0^{(q)}(T_1 R_0)}{q!} [T_1 h \cos(k_0 z)]^q, \tag{36}$$

$$N_0(T_1 R(z)) = \sum_{q=0}^{\infty} \frac{N_0^{(q)}(T_1 R_0)}{q!} [T_1 h \cos(k_0 z)]^q. \tag{37}$$

Substituting Eqs.(36) and (37) into Eq.(35), we obtain

$$\boldsymbol{D} \cdot \boldsymbol{A} = \sum_{n=-\infty}^{\infty} D_{mn} A_n = 0, \quad m = 0, \pm 1, \pm 2, \cdots \pm n, \tag{38}$$

where $\boldsymbol{A}$ is a column vector with elements A_n, and $\boldsymbol{D}$ is a matrix with elements D_{mn} obtained from the integral in Eq.(35).

$$D_{mn} = [1 + (n-m)Q_n](R_n C^{\mathrm{J}}_{mn} + T_n C^{\mathrm{N}}_{mn}), \quad (39)$$

where

$$Q_n = \frac{k_0 k_n}{(\omega^2/c^2) - k_n^2}, \quad (40)$$

$$C^{\mathrm{J}}_{mn} = \sum_{q=0}^{\infty} \frac{(T_1 h)^{2q+|n-m|} J_0^{(2q+|n-m|)}(T_1 R_0)}{2^{2q+|n-m|} q!(q+|n-m|)!} \quad (41)$$

$$C^{\mathrm{N}}_{mn} = \sum_{q=0}^{\infty} \frac{(T_1 h)^{2q+|n-m|} N_0^{(2q+|n-m|)}(T_1 R_0)}{2^{2q+|n-m|} q!(q+|n-m|)!}. \quad (42)$$

Equation (42) represents an infinite set of linear equations. The dispersion relation for the plasma-filled RTWT is expressed as a determinant equation

$$|\boldsymbol{D}| = 0. \quad (43)$$

4. Numerical computation and analysis

From the numerical computation for dispersion equation (43), we can analyse the dispersion characteristics of the slow wave structure. In the case of infinitesimally small beam density ($\omega_{\mathrm{b}} = 0$), the oscillation frequency $\omega/2\pi$ is real for a real-valued wave number k_z. Only TM_{01} mode is taken into account, and the dispersion curves of a whole period calculated using a 7×7 determinant are shown in Figs.2–5.

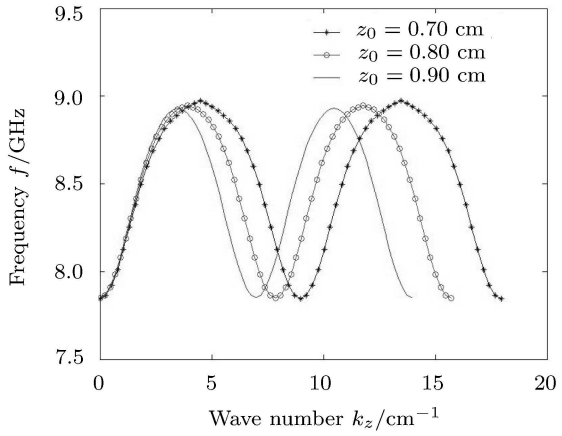


Fig.2. Cold dispersion relation for various corrugation periods.

In Fig.2, the parameters are $n_{\mathrm{p}} = 2.0\times10^{11}$ cm^{-3}, $R_0 = 1.60$ cm, $h = 0.55$ cm. Figure 2 shows the cold dispersion relation for various corrugation periods. As the corrugation period increases, the period of the dispersion curve diminishes accordingly.

In Fig.3, the parameters are $n_{\mathrm{p}} = 2.0\times10^{11}$ cm^{-3}, $R_0 = 1.60$ cm, $z_0 = 0.80$ cm. Figure 3 shows the cold dispersion relation for various corrugation amplitudes. It can be found that the dispersion curves get sharper and the group velocities of the electromagnetic wave increase due to the diminished corrugation amplitude.

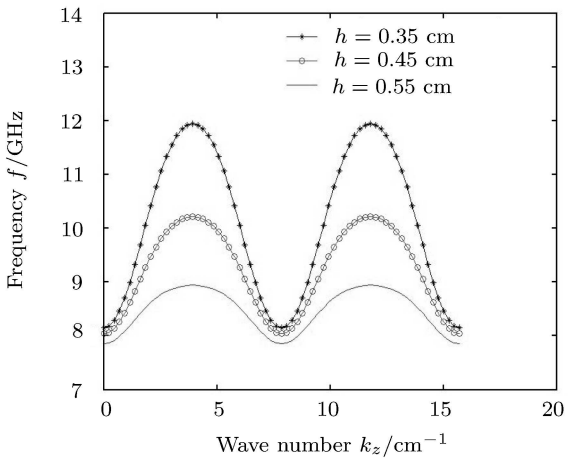


Fig.3. Cold dispersion relation for various corrugation amplitudes.

In Fig.4, the parameters are $n_{\mathrm{p}} = 2.0\times10^{11}$ cm^{-3}, $h = 0.55$ cm, $z_0 = 0.80$ cm. Figure 4 shows the cold dispersion relation for various values of average radius. It can be seen that the dispersion curves rise higher and the group velocities of the electromagnetic wave decrease due to the diminishing of average radius.

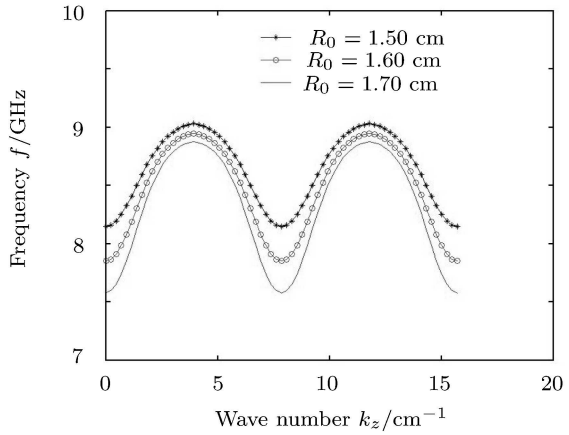


Fig.4. Cold dispersion relation for various average radius.

In Fig.5, the parameters are $R_0 = 1.60$ cm, $h = 0.55$ cm, $z_0 = 0.80$ cm. Figure 5 shows the cold

dispersion relation for various plasma densities. As the plasma density increases, the dispersion curves rise higher and the group velocities of the electromagnetic wave decrease. The result shows that the operating frequency of the tube increases, but the bandwidth narrows.

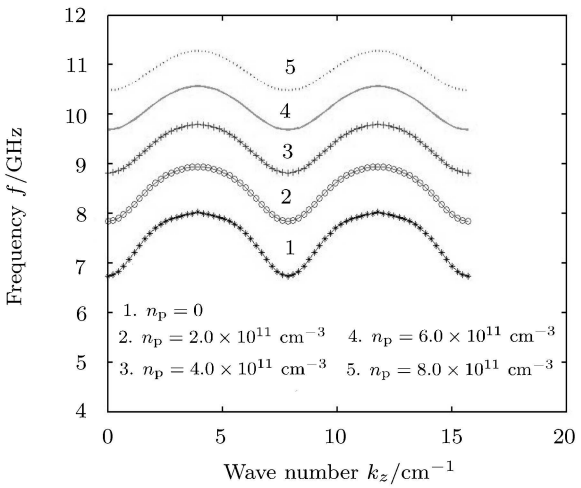


Fig.5. Cold dispersion relation for various plasma densities.

As the presence of electron beam is taken into account, the wave number k_z is complex and the gain of the RTWT is given by

$$G = -9.54 + 10\log[\mathrm{e}^{2\mathrm{Im}(k_z)z}], \qquad (44)$$

where $\mathrm{Im}(k_z)$ is the imaginary part of k_z, and z is the length of the interaction area. To obtain k_z, $D(\omega, k_z)$ are expanded in Taylor series about $k_z = k_{z0}$,

$$D(\omega, k_z) \approx D(\omega, k_{z0}) + (k_z - k_{z0})\frac{\mathrm{d}D}{\mathrm{d}k_z} = K. \qquad (45)$$

This is an equation of circle with radius $|K|$ on the complex plane. For a given ω, the solution can be found at the centre of the contour circle lines of $|D|$.

In the following calculations, the parameters of the SWS are the same as those in Fig.5; the electron beam current is 1.5 kA, and the total length of the interaction area is 9.6 cm, the inner radius of the electron beam $R_b = 0.70$ cm, and the outer radius of it $R_c = 0.90$ cm.

Figure 6 shows the dispersion relations of the SWS driven by an electron beam. Figure 7 shows the relations between the gain of the SWS and the frequency. For each plasma density in Figs.6 and 7 the electron beam voltage is chosen to maximize the gain at a frequency of 8.05 GHz. Thus, the electron beam voltage corresponding to the three plasma densities $n_p = 1.0 \times 10^{11}/\mathrm{cm}^3$, $n_p = 5.0 \times 10^{10}/\mathrm{cm}^3$ and $n_p = 0$ are 225, 168 and 144 kV, respectively. It is found from Fig.6 that there is a visible difference between the dispersion relation of the SWS driven by an electron beam and the cold dispersion relation. The phase velocities of the electromagnetic waves become slowing down after the electron beam is injected into the system. From Fig.7 it can be seen that the presence of plasma enhances the peak gain of the tube. As the plasma density increases, the peak gain and the frequency of the peak gain also increase, but at low frequencies (less than the frequency corresponding to the peak gain of the tube in vacuum) the gain of the tube decreases.

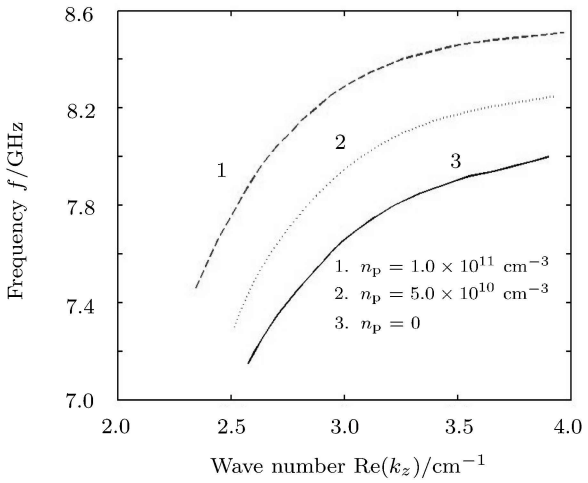


Fig.6. Dispersion curves of the SWS driven by an electron beam for three different plasma densities.

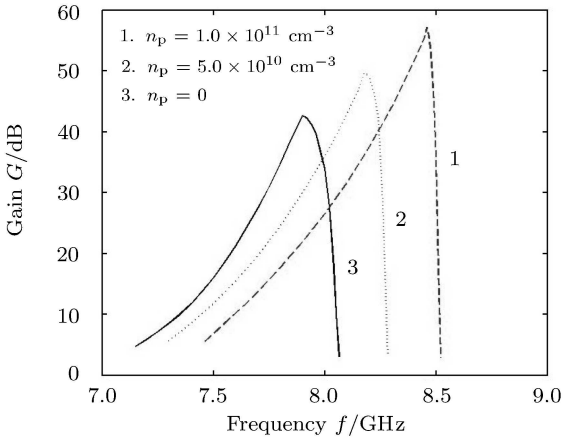


Fig.7. Gain versus frequency for three different plasma densities.

Figure 8 shows the gain versus plasma density for a given frequency 8.05GHz. For each plasma den-

sity the required beam voltage varies between 142 and 220kV in order to achieve a maximum gain. It can be found that there is a best plasma filling density to achieve a maximum gain.

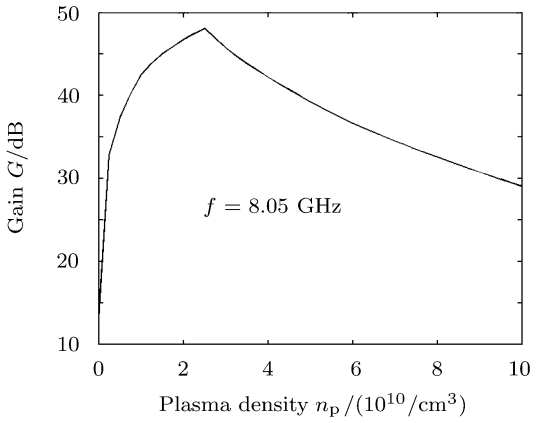


Fig.8. Gain versus plasma density for a given frequency.

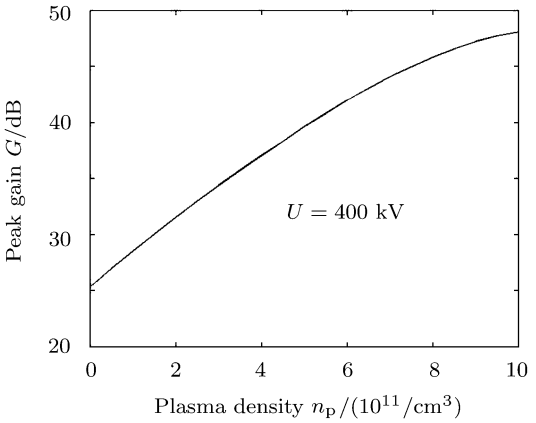


Fig.9. Peak gain versus plasma density.

Figure 9 shows the relation between plasma density and the peak gain of the tube driven by an electron beam of high voltage $U = 400$ kV. As the plasma density increases, the peak gain of the tube is enhanced correspondingly, but the rising trend becomes gradually slowing down.

5. Conclusions

According to the above theoretical analysis, some useful results are obtained. 1) The parameters of the slow wave structure will dramatically affect the dispersion relation of the tube. 2) There is a visible difference between the dispersion relation of the SWS driven by an electron beam and the cold dispersion relation. 3) The presence of plasma in the slow wave structure will increase the operating frequency of the TM_{01} mode and the peak gain of the tube. 4) As the plasma density increases, at low frequencies (less than the frequency corresponding to the peak gain of the tube in vacuum) the gain of the tube decreases. 5) For a given frequency, there is a best plasma filling density to achieve a maximum gain. 6) For a given very high voltage, as the plasma density increases, the peak gain of the tube is enhanced, but the rising trend becomes slow gradually.

Certainly, the above results are achieved on the basis of the assumption that B_0 is infinitely strong. They are only preliminary studies in theoretical research domain. They need to be approved in experiment in the future.

References

[1] Sshiffler D, Nation J A and Graham S K 1990 *IEEE Trans. Plas. Sci.* **18** 546
[2] Sawhney R, Maheshwari K P and Choyal Y 1993 *IEEE Trans. Plas. Sci.* **21** 609
[3] Zavyalov M A, Mitin L A, Perevodchikov V I, Tskhai V N and Shapiro A L 1994 *IEEE Trans. Plas. Sci.* **22** 600
[4] Nusinovich G S, Carmel Y and Antonsen T M Jr 1998 *IEEE Trans. Plas. Sci.* **26** 628
[5] Kobayashi S, Antonsen T M Jr and Nusinovich G S 1998 *IEEE Trans. Plas. Sci.* **26** 669
[6] Xie H Q, Li C Y, Yan Y and Liu S G 2003 *Acta Phys. Sin.* **52** 914 (in Chinese)
[7] Xie H Q, Liu P K, Li C Y, Yan Y and Liu S G 2004 *Acta Phys. Sin.* **53** 3114 (in Chinese)
[8] Xie H Q , Yan Y and Liu S G 2002 *High Power Laser and Particle Beams* **14** 114 (in Chinese)
[9] Zhang Y, Mo Y L, Xu R M, Yan B and Xu X Q 2005 *Acta Phys. Sin.* **54** 5239 (in Chinese)
[10] Li W, Wei Y Y, Xie H Q, Liu S G and Gong M L 2003 *Chin. Phys.* **12** 532
[11] Xie H Q and Liu P K 2006 *Acta Phys. Sin.* **55** 2397 (in Chinese)
[12] Zhang J, Zhong H H and Luo L 2004 *IEEE Trans. Plas. Sci.* **32** 2236
[13] Goebel D M, Butler J M, Schumacher R W, Santoru J and Eisenhart R L 1994 *IEEE Trans. Plas. Sci.* **22** 547
[14] Ali M M, Minami K, Amano S, Ogura K and Watanabe T 1991 *J. Phys. Soc. Japan* **60** 2655
[15] Ali M M, Ogura K and Minami K 1992 *Phys. Fluids* B **4** 1023
[16] Carmel Y, Lou W R, Antonsen T M, Rodgers J, Levush B, Destler W W and Granatstein V L 1992 *Phys. Fluids* B **4** 2286
[17] Liu S G, Barker R J, Zhu D J, Yan Y and Gao H 2000 *IEEE Trans. Plas. Sci.* **28** 2135
[18] Liu S G, Barker R J, Yan Y and Zhu D J 2000 *IEEE Trans. Plas. Sci.* **28** 2152
[19] Gao H and Liu S G 2000 *Chin. Phys.* **9** 274